Multi-Temporal Assessment of Desertification Degree in Kaita and Mashi Areas of Katsina state, Nigeria using Feature-Space Technique

AbdulAzeez Onotu Aliyu[1], Adamu Bala[1,2], Swafiyudeen Bawa[1], Ebenezer Ayobami Akomolafe [1], and Fatima Tijjani Ahmad [1]
[1]Department of Geomatics, Ahmadu Bello University, Zaria, Kaduna State, Nigeria.
[2]School of Geography and Information Engineering, China University of Geosciences, Wuhan, 430074, PR China.
*Correspondence: abdulonotu@gmail.com

Keywords: Albedo, Desertification Degree Index, Feature-space, NDVI, Regression analysis

Abstract

Desertification poses a severe environmental threat in Katsina state, northern Nigeria. While previous studies have assessed desertification in Katsina state and Nigeria, the feature-space technique, which identifies location-specific indicator pairs, remains unexplored. This study conducted a spatio-temporal assessment (1999, 2009, 2024) using Landsat imagery to map desertification degree. Assessment indices for desertification such as albedo, LST, NDVI, SAVI, MSAVI, and MNDWI were derived. Regression analysis was conducted to identify significant negative correlations between albedo or LST and other indices. Results showed the albedo-NDVI pair had the consistent significant negative correlation (r = 0.62, 0.51, 0.63), thus leading to the construction of an albedo-NDVI feature-space and the computation of a Desertification Degree Index (DDI). The DDI classified the area into three levels: desertification, potential desertification, and non-desertification (vegetation/water). The DDI maps indicated that desertification extent increased between 1999 and 2009 but declined slightly by 2024, while potential desertification expanded continuously with 40.37%, 41.44% and 47.33% in 1999, 2009 and 2024 respectively. Non-desertification extent (vegetation) decreased steadily, reflecting increasing anthropogenic and climatic pressures. Expansion rate analysis showed that potential desertification is the fastest-growing class at 0.69% per annum, thus highlighting its role as a precursor to full desertification. The DDI maps were robustly validated using Soil Organic Carbon, which demonstrated moderate but significant negative correlations (r = 0.51, 0.593, 0.563 for 1999, 2009, 2024), thus confirming the ecological relevance of the DDI. The feature-space technique is effective in that it has provided strong correlated indicators that are location-based to the study area.

1. INTRODUCTION

1.1 Background to the Study

Desertification is defined as the land degradation in arid, semi-arid, and dry sub-humid areas caused by climatic variations and human activities (UNCCD, 1994). Desertification is the consequence of the interplay of environmental factors (topography, climate, soil and vegetation) and anthropic factors such as deforestation, overgrazing and inappropriate management practices (Bouabid et al., 2010, and Salvati et al., 2016, in Boultaka et al., 2023). The phenomenon affects very large areas of the world and can result in irreversible loss of land productivity (Wijikosum, 2016). Nevertheless, it has impacts on the human population as it triggers famine, disease, and population relocation (Elijah and Ikusemoran, 2017).

Desertification is a global concern, particularly in dryland regions like northern Nigeria (Remigios, 2010), which lies within the Sudano-Sahelian agro-ecological zone. The rate of desertification rate in northern Nigeria is estimated at 0.6 km per year, with 350,000 hectares lost annually (Nwafor, 2006; Tercula, 2015 in James et al., 2018). In Nigeria, desertification affects 15 states, of these states, desertification is critical in 11 states, known as the frontline states, namely: Adamawa, Borno, Bauchi, Gombe, Katsina, Jigawa, Kano, Kebbi, Sokoto, Yobe and Zamfara (Odiogor, 2010). These eleven states are bordered by the Republic of Niger (Mamadu and Kuje, 2016). Katsina state experiences the most severe impacts of desertification and is especially vulnerable due to over 75% of its population relies on agriculture and its location is in the extreme north of Nigeria bordering the Republic of Niger (Saulawa et al., 2018).

While Abdulrashid (2017), James et al. (2018), and Saulawa et al. (2018) analyzed desertification across Katsina state, their findings showed that desertification is prominent in the north. The studies treated the northern Katsina as a single generalized zone and did not account for specific indicators that have strong relationship in defining desertification degree. Kaita and Mashi, located at the extreme north of Katsina state and sharing an international border with the Republic of Niger, represent a unique and highly vulnerable frontline of desertification processes in Katsina state. However, desertification indicators that are strongly correlated and locally meaningful in Kaita and Mashi have not been analyzed.

Addressing desertification requires understanding its extent and degree. Methods for assessing desertification include direct observation (questionnaire), mathematical models, other indicators (Ladisa et al., 2012; Sepehr et al., 2007 in De Pina Tavares et al., 2014), and remote sensing. Remote sensing is especially valuable for monitoring biophysical, climatic, geological, and hydrological indicators over large areas (Rivera-Marin et al., 2022). It is a chief source of data for biophysical, climatic, geological, hydrological, and topographical indicators of desertification.

Previous studies that applied remote sensing to assess desertification in northern Nigeria have used supervised classification and Normalized Difference Vegetation Index (NDVI) analyses (e.g. Musa and Shaib, 2010 in Yobe state; Yelwa and Eniolorunda, 2012 and Aliyu, 2015 in Sokoto state) and Cellular (e.g. Falaki et al., 2020 in Jibia, Katsina state). However, the supervised classification and NDVI analysis focus on the visual presence of certain landcovers (e.g. bare-land or rocky surface and vegetation). The Cellular Automata predict land use and landcover change but not desertification degree. Additionally, Abdulrashid (2017) and Saulawa et al. (2018) used questionnaires to elicit the inhabitants of Katsina state on the impact of desertification on livelihoods. However, the study focused only on the perception of the inhabitants, but not the biophysical factors of the environment.

Another widely used desertification model is the Mediterranean Desertification and Land Use (MEDALUS) model, which uses climate, soil, vegetation, and management factors to map desertification degree. This model has been applied in Katsina state (James et al., 2018), Jigawa state (Ahmed et al., 2020) of Nigeria, and the Niger Basin (Ogbue et al., 2024). However, some of the MEDALUS desertification indicators may not strongly correlate with local desertification degree in Katsina State, possibly decreasing their detection capability.

The feature-space technique is an advanced remote sensing approach that plots biophysical indicators with strong relationships with each other to distinguish land cover types and desertification degree based on their spectral characteristics in dryland environment (Ding et al., 2014). By plotting indices such as Land Surface Temperature (LST) or albedo versus vegetation and water indices (e.g., NDVI), it is possible to identify desertification degree that may not be apparent from simple image interpretation. A key advantage of the feature-space technique is its ability to exclude less-relevant indicators by requiring strong negative correlations between indicator pairs (Sun and Kafatos, 2007). The LST is the "radiative skin temperature" of the Earth's surface, which is the temperature that a surface (soil, vegetation, water, built structures) emits as sensed from satellite thermal infrared sensors. Albedo is a measure of incoming solar radiation that is reflected back by a surface. It ranges from 0 (complete absorption, like a perfectly black surface) to 1 (total reflection, like fresh snow) and is unitless. It is a vital climate variable because it affects the Earth's energy budget (Liang et al., 2013; Yang et al., 2022). The vegetation indices measure the vitality and greenness of vegetation of an area, while water index measures the amount of water in open ground. The Desertification Degree Index (DDI) is a quantitative metric derived from remote sensing data that characterizes and maps desertification severity within a given area. It is computed by analyzing the feature space relationship between two or more biophysical indices that exhibit a strong negative correlation.

Feature-space analysis has proven effective in desertification mapping elsewhere. Anh et al. (2006) used LST vs. NDVI in Vietnam; Ma et al. (2011), Lamqadem et al. (2018), and Salih et al. (2021) used albedo vs. NDVI in Morocco, China, and Saudi Arabia, respectively. Wei et al. (2018) used multiple feature space relationships and found that albedo vs. NDVI performed second only to albedo vs. Tasseled Grain Soil Index (TGSI). Wu et al. (2019) and Wen et al. (2020) applied albedo vs. Modified Soil Adjusted Vegetation Index (MSAVI) in China. The study of Wu et al. (2019) applied the feature-space from 2002 to 2017 of three-year interval. Yousef and Alkhaqani (2020) used NDVI vs Spectral Principal Component (SPC) for desertification detection in Iraq. These studies used the feature-space to compute a Desertification Degree Index (DDI) for desertification assessment, which successfully classified areas into distinct levels based on their spectral characteristics. While the existing studies have provided a basis for understanding the feature-space in desertification mapping, significant gaps remain, especially in the context of Nigeria.

Despite these successes, most previous studies use single-date analysis, while few studies used short temporal intervals (1-3 years), which often does not capture subtle or slow processes. Ongsomwang (2007) recommended a minimum ten-year gap for meaningful change detection. This principle is extensively backed in the literature, since subtle processes such as desertification and land degradation are best identified over decadal intervals to ensure reliability and reduce temporal noise (Hansen et al., 2013; Kennedy et al., 2014; Zhu and Woodcock, 2014). Furthermore, this current study is unaware of any previous studies that has explored the feature-space technique to assess desertification degree in Katsina state or Nigeria at large. It is in the light of the above, this study aims to fill this gap by applying a multi-temporal feature-space technique over more than two decades (1999, 2009, 2024) in Kaita and Mashi Local Government Areas (LGAs) of Katsina state, Nigeria. The specific objectives of the study are to: (i) derive the desertification assessment indices for 1999, 2009, and 2024; (ii) determine which indices have strong negative correlation with albedo and/or LST; (iii) construct a feature space of the selected indices to derive the Desertification Degree Index (DDI) for mapping spatial distribution and temporal change of desertification degree in Kaita and Mashi areas; and (iv) validate the DDI. The rationale for evaluating many desertification assessment indices was to test which indicators are locally meaningful, and avoid reliance on irrelevant or weakly correlated indicators. In addition, the causes, indicators, and degree of location-based process such as desertification can vary greatly across regions (Salvati et al., 2016; Rivera-Marín et al., 2022) as a result of spatial heterogeneity. Furthermore, the idea of multi-temporal analyses aided to ascertain the rate of change and expansion rate of the desertification degree. The study is historical, descriptive, and explorative.

1.2 Study Area

The study covered Kaita and Mashi are two Local Government Areas (LGAs) of thirty-four LGAs of Katsina State, north-western Nigeria. They are located between longitudes 7°30′00″E to 8°10′21.96″E and latitudes 12°55′8.7″N to 13°20′34.68″N. it is characterized by a cold-dry semi-arid climate, Sudan savannah vegetation. It is composed of sandy loam soils. The land area is about 182, 974.47 ha. The population is 280,824, 391,257 and 614,020 in 1999, 2009, and 2024 (NPC, 2006).

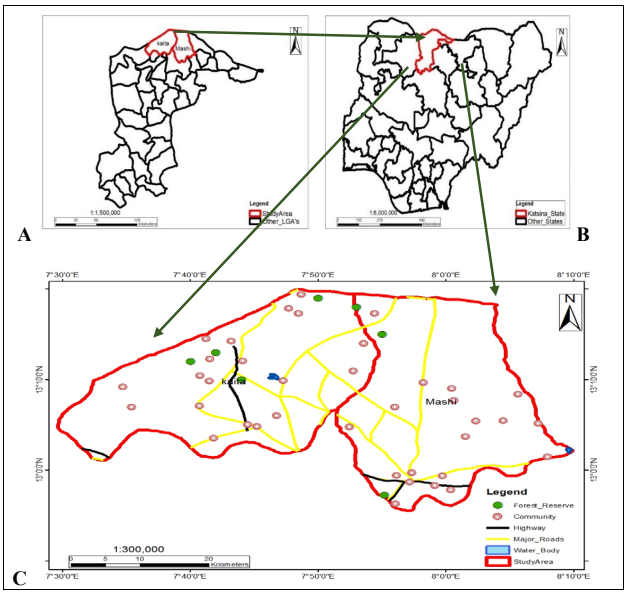

Figure 1: Inset map: (a) Nigeria showing Borno State. (b) Katsina state showing Monguno L.G.A. (c) Kaita and Mashi (Study area)

2. MATERIALS AND METHODS

This section describes the data sources, pre-processing, indices derivation, regression analysis, and construction of the feature-space model. Figure 2 presents the overall workflow.

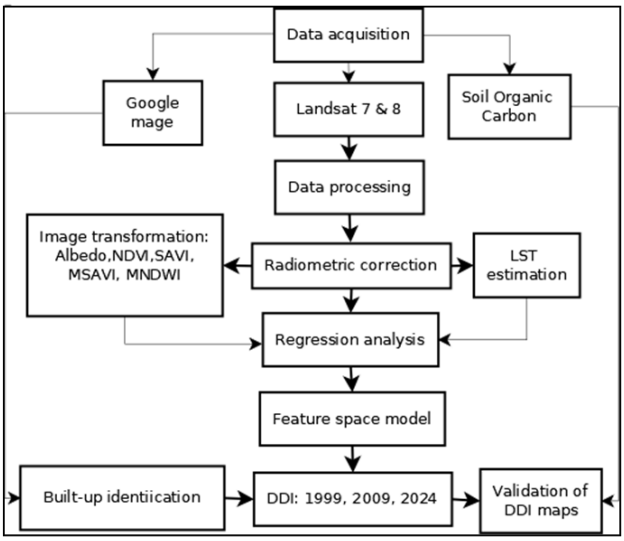

Figure 2: Workflow diagram of the study

2.1 Datasets and Sources

Table 1 summarizes the datasets. Landsat 7 ETM+ (1999, 2009) and Landsat 9 OLI/TIRS (2022) images were acquired from the United States Geological Survey (USGS) for December. December marks the transition from the rainy to the dry season in the study area and to avoid the exaggeration of vegetation

S/N	Data Name	Year	Product ID	Source
1	Landsat 7	1999 & 2009	LE07_L1TP_189051_19991206_20170215_01_T1 (1); LE07_L1TP_189051_20091201_20161218_01_T1	United States Geological Survey (USGS)
2	Landsat 8	2024	LC08_L1TP_189051_20241218_20241227_02_T1	
3	Soil Organic Carbon	2024	Nil	https://soilgrids.org/
4	Google image	2024	Nil	Google Earth
5	Administrative shapefile	Nil	Nil	https://www.diva-gis.org/Data

Table 1: Datasets and their characteristics

and dry season. The Landsat images were in Digital Number (DN) scale. The 2024 image scene and land cloud cover of 0.11%, while the 1999 and 2009 image had none. Soil Organic Carbon (SOC) was acquired in 250m cell size for validating the DDI maps. Google Earth image was also used for ancillary data.

2.2 Data Processing

2.2.1 Radiometric correction

All Landsat bands (excluding thermal bands) were converted from Digital Numbers (DN) to Top-of-Atmosphere (TOA) radiance and then to surface reflectance using the Semi-Automatic Classification Plugin (SCP) in QGIS. Surface reflectance is essential for deriving consistent indices, as it better represents true land cover differences (Aliyu et al., 2022). Corrections accounted for Earth–Sun distance, atmospheric scattering and absorption, bandwidth, and solar illumination angle.

2.2.2 Image transformation (Index derivation)

For clarity, the desertification indicators provide information about and describes the state of an environment or phenomenon (desertification), while the desertification indices are computed numerical representations of the desertification indicators. The following indices were computed (see Table 2 for formulas and references): NDVI, Soil Adjusted Vegetation Index (SAVI), Modified Soil Adjusted Vegetation Index (MSAVI), LST, Modified Normalized Difference Water Index (MNDWI) and albedo in Raster Calculator tool in ArcMap v10.8. Albedo was computed as a weighted sum of reflectance in selected bands to quantify surface reflectance variability related to soil moisture and vegetation cover.

S/N	Expression	Reference
1.	$NDVI = \frac{NIR - RED}{NIR + RED}$	Carlson *et al.* (1997)
2.	$SAVI = \frac{NIR - RED}{NIR + RED + L} * (1 + L)$	Haboudane *et al.* (2004)
3.	MSAVI = $\frac{2NIR + 1 - \sqrt{(2NIR = 1)^2 - 8(NIR - R)}}{2}$	Qi *et al.* (1994)
4.	$MNDWI = \frac{GREEN^2 - NIR}{GREEN + NIR}$	Xu (2006)
5.	$Albedo = 0.356\,BLUE + 0.13\,RED + 0.373\,NIR + 0.0855\,SWIR1 + 0.072\,SWIR2 - 0.0018$	Guo *et al.* (2019)

Table 2: Mathematical expressions for the desertification indices and their references.

Note: L = soil brightness correction factor (taken as 0.5) (Huete et al., 2002). R = red; NIR = near infrared; and SWIR = short wave near infrared.

2.2.3 Land Surface Temperature (LST) estimation

LST was estimated using the split-window method, which computes the proportion of vegetation (from NDVI), Land Surface Emissivity (LSE), and Top-of-Atmosphere (TOA) brightness temperature. The split-window was used because it requires no information of atmospheric parameters and is computationally easy. Details of the mathematical expressions are reported in Aliyu et al. (2019) and Sajib and Wang (2020). Thermal bands (band 6 for Landsat 7 and band 10 for Landsat

8) were converted to at-sensor radiance and brightness temperature.

2.3 **Data Analysis**

2.3.1 **Sample point generation**

Systematic random sampling was used to generate 1000 × 1000m grid points across the study area. This was necessary for the regression analysis. The 1000m grid dimension creates a balance between computational efficiency and sufficient spatial detail for Landsat data at 30m cell size. 2100 sample points were generated for each assessment index. Thereafter, the raster values of the of derived indices were aligned and overlaid to enable extraction of the pixel values at common points into the sample points. Extract values to point tool in ArcMap v10.8 was used.

2.3.2 **Regression analysis**

After the extraction of the values of the derived indices into the sample points, simple linear regression was performed in Excel using the XLSTAT add-in to ascertain pairs of indices that are suitable (show strong correlation) for the construction of feature-space. Albedo and LST were treated as dependent variables, while NDVI, SAVI, MSAVI, and MNDWI were independent variables. Coefficients of determination (R^2) and correlation (r) values were calculated to assess strength and direction of the relationships. Pairs with strong negative correlations were selected for feature-space construction.

2.3.3 **Feature-space construction**

Based on regression results, the albedo–NDVI pair, which consistently showed strong negative correlation across all years (1999, 2009, 2024), was chosen. Feature-space plots were constructed with albedo on the y-axis and NDVI on the x-axis for years 1999, 2009, and 2024. The plot was constructed using the spectral plot tool in ENVI v5.2.

To map the desertification severity, the slope of the regression analysis was used to compute the Desertification Degree Index (DDI). The DDI for desertification using remote sensing derived indices is based on the albedo-NDVI feature-space plot that was constructed by Zeng et al. (2006) and has been widely used by Xiulian, 2017; Wu et al., 2019; Wen et al., 2020; Yousef and Alkhaqani, 2020. The mathematical expression is shown in Equation 8.

$$DDI = a \times NDVI\text{-}Albedo \quad \text{Eqn. 6}$$

Where, a = slope of the regression equations of albedo-NDVI for 1999, 2009, 2024, which are 0.434, 0.455, and 0.279 respectively. After determining the slope of the equations, the DDI was computed using raster calculator and the Jenks natural breaks classification in ArcMap v10.8 to classify the DDI into 5 levels: desertification (bareland, rock outcrops), potential desertification (cultivated, uncultivated land), non-desertification (vegetation), non-desertification (waterbody). After this, metrics such as expansion rate was computed (see Equations 9) as post-DDI analysis.

$$ER\ (\%/year) = \frac{R-P}{P} \times \frac{1}{T} \times 100\% = RC \times \frac{1}{T} \quad \text{Eqn. 7}$$

2.3.4 Validation of DDI

A few studies that validated DDI largely relied on pixel-based validation techniques, such as confusion matrix, kappa coefficient, producer's and user's accuracies, and Area Under Curve (AUC) analysis.

While these techniques provide useful information on the thematic or positional accuracy of desertification classes, they primarily represent a physical visualization of pixel placement or misplacement relative to a reference image, without necessarily validating the biophysical robustness of the index. Studies that used this approach are Lamqadem et al. (2018) and Wei et al. (2018). In contrast, Wu et al. (2019) employed a process-oriented validation by correlating Semi-Arid Steppe Desertification Index (SASDI) with Soil Organic Matter (SOM) in China. In addition, Salunkhe et al. (2018) correlated the derived Index map with soil chemical properties, particularly Soil Organic Matter (SOM) and Cation Exchange Capacity (CEC), thereby linking the index to actual chemical soil properties. Therefore, the decrease in the SOM or CEC of soil will accelerate desertification and vice versa.

However, few studies have extended this validation approach to Soil Organic Carbon (SOC), despite its recognized importance as a critical indicator of soil fertility. SOC, being the dominant fraction of SOM, it constitutes about 58% of SOM (Rawls et al., 2003) and is more directly quantifiable and serves as a reliable measure of soil health and degradation status (Lal, 2004).

It is expected that a strong inverse correlation will exist between the DDI value (where higher values indicate severe desertification) and SOC (where lower values indicate poor soil health). Therefore, this study validated the derived DDI by analyzing its statistical correlation with SOC. To validate the DDI, 450 sample points were generated along each DDI class (desertification and potential desertification) using stratified sampling. The stratified sampling ensured correct representation of the sample points for each DDI class. A total of 900 sample points were generated. Then the derived DDIs and the SOC were aligned and overlaid to enable extraction of the pixel values at common points into the 900 sample points. Extract values to point tool in ArcMap v10.8 was used. XLSAT add-in of Excel was used for the statistical analysis.

3.1 Results and Discussion

3.1.1 Derived albedo, vegetation and water indices, and estimated LST for 1999, 2009, and 2024

Having derived the albedo, vegetation and water indices, and estimated the LST from the remotely sensed imagery, Table 3 summarizes descriptive statistics i.e. minimum, maximum and Coefficient of Variation (CV) of the derived vegetation and water indices and LSTs for 1999, 2009, and 2024. The CV details the spread or dispersion of the indices across the study area. All the derived indices had CVs less than 1 for 1999, 2009, and 2024, which indicated low spread throughout the study area. However, the CVs of the NDVI were 0.15, 0.13, and 0.18 for 1999, 2009 and 2024 respectively. The NDVI of 2024 had a higher spread, followed by 1999 and then 2009. Since the CVs of the NDVI were higher than the SAVI and MSAVI, it can be deduced that the NDVI had a better spread across the

study area. More so, the NDVI had higher maximum values of 0.545, 0.47 and 0.86 for 1999, 2009, and 2024 respectively, which were higher than the SAVI and MSAVI. The raster of the derived albedo, vegetation and water indices, and estimated LST for 1999, 2009, and 2024 are shown in Figures 3 (A-F), 4 (A-F), and 5 (A-F) respectively. The minimum and maximum values of the indices are shown in different colors.

2024	**C.V.**	0.03	0.12	0.18	0.14	0.14	0.08
	Max.	40.328	0.483	0.86	0.637	0.671	0.924
	Min.	20.351	0.195	-0.61	-0.326	-0.243	-0.753
2009	**C.V.**	0.02	0.07	0.13	0.12	0.11	0.07
	Max.	35.011	0.445	0.470	0.366	0.352	0.617
	Min.	17.091	0.085	-0.190	-0.106	-0.080	-0.460
1999	**C.V.**	0.03	0.08	**0.15**	0.13	0.12	0.08
	Max.	39.504	0.438	0.545	0.389	0.375	0.705
	Min.	18.557	0.103	-0.239	-0.170	-0.153	-0.569
Year	**Index**	LST	Albedo	NDVI	SAVI	MSAVI	MNDWI
	S/N	1	2	3	4	5	6

Table 3: Statistics of the derived indices for 1999, 2009, and 2024.

NOTE: Coefficient of Variation: CV=SD/Mean. CV < 1 = low dispersion or variance; CV ≥ 1 = high dispersion; and SD = Standard Deviation.

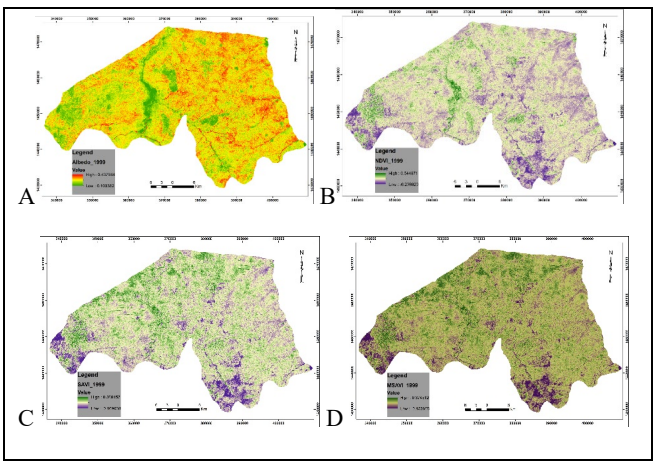

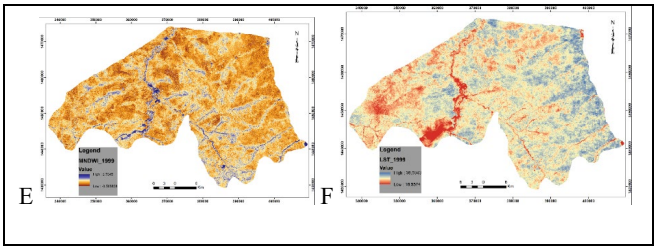

Figure 3: Derived indices for 1999. A: Albedo; B: NDVI; C: SAVI; D: MSAVI; E: MNDWI; F: LST.

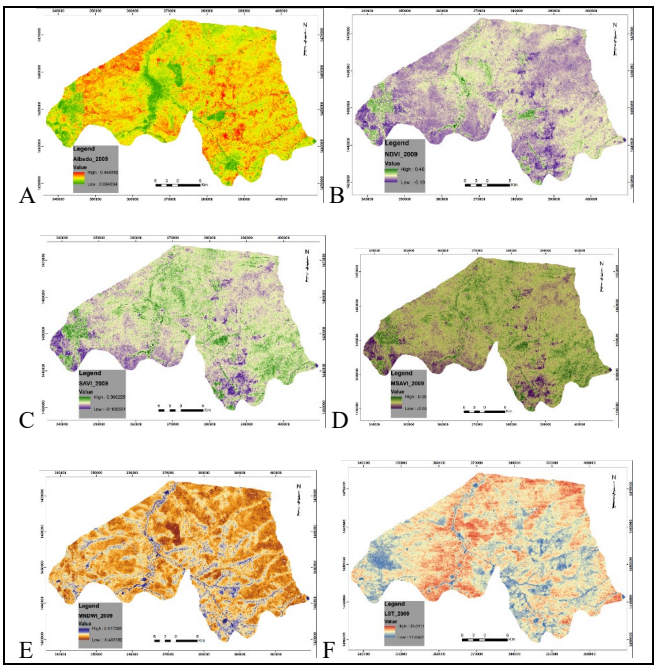

Figure 4: Derived indices for 2009. A: Albedo; B: NDVI; C: SAVI; D: MSAVI; E: MNDWI; F: LST.

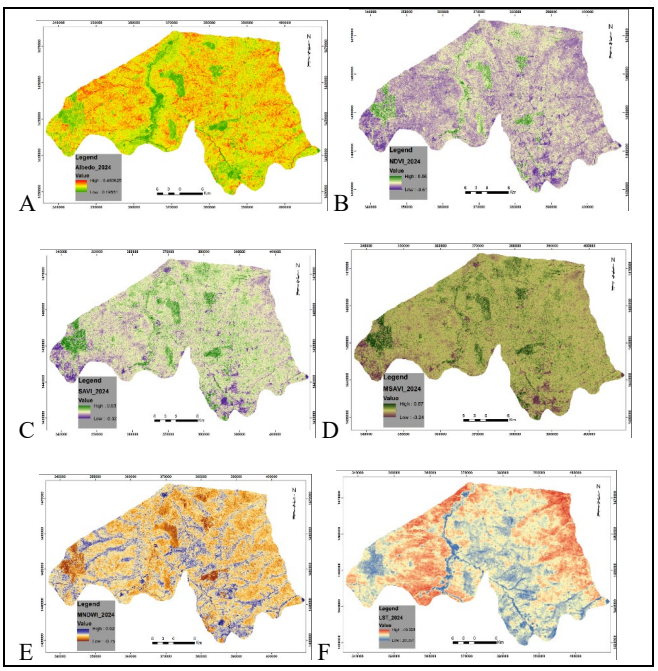

Figure 5: Derived indices for 2024. A: Albedo; B: NDVI; C: SAVI; D: MSAVI; E: MNDWI; F: LST

Combining the CVs and maximum values of the NDVI, though despite its low CV, it can be deduced that the NDVI had a better spread across the study area compared to its counterparts, and can be regarded as the appropriate index for delineating vegetation in the study. The low spread of the vegetation indices across the study area for the study years could be attributed to low vegetation in the study area and the period or season in which the imagery was collected.

3.2 Regression Analysis of Desertification Indices

3.2.1 Relationship between albedo and NDVI, SAVI, MSAVI, MNDWI

To ascertain pairs of indices that are suitable for the construction of feature-space, Table 4 shows equations of the linear regression and coefficients of correlation for 1999, 2009, and 2024 respectively. Albedo had a negative correlation with the NDVI, SAVI, and MSAVI for 1999, 2009, and 2024. It implied that higher vegetation cover was associated with low albedo vice versa. For the strength of the correlation, albedo had consistently normal negative correlations with only the NDVI across all years (r = 0.62 in 1999, 0.51 in 2009, and 0.63 in 2024). The albedo-NDVI correlation was statistically and highly significant at 95% interval (p-values < 0.05). A 95% confidence interval was adopted, and is consistent with standard practice in environmental and remote sensing studies (Li et al., 2013; Karnieli et al., 2010). Other indices (SAVI, MSAVI) also had negative correlations but were slightly weaker correlations (See Table 3). According to Cohen et al. (2013), correlation coefficient (r), with 0.31-0.5 represents a weak correlation, 0.51-0.7 represents a normal correlation, 0.71- 0.90 represents a strong correlation, and 0.91-1.0 represents a very strong correlation. Additionally, albedo had negative correlations with MNDWI for 1999 and 2009, but positive correlation in 2024. Though the correlations between the albedo and the MNDWI were weak and inconsistent.

3.2.1 Relationship between LST and NDVI, SAVI, MSAVI, MNDWI

For the LST correlation with the indices, LST had weak negative correlations with the NDVI, SAVI, MSAVI and MNDWI for 1999, 2009, and 2024. However, LST had a positive normal correlation with only the MNDWI in 2009 (See Table 4). While it is expected that the LST has a negative correlation with vegetation, the weak correlation is unexpected. In general, LST exhibited weak and less consistent correlations overall. Since the albedo and the NDVI had a consistent and significant correlation throughout the years, the pair of the albedo-NDVI was chosen and used for the construction of the feature-space and computation of the DDI. The scatterplots of the albedo-NDVI for 1999, 2009, and 2024 is shown in Figure 6.

This relationship of the albedo-NDVI aligns with theoretical expectations, where higher vegetation cover (NDVI) is associated with reduced surface reflectance (albedo), which is indicative of healthy soils and low desertification sensitivity. Similar findings have been reported by Ma et al. (2011) in Morocco and Salih et al. (2021) in Saudi Arabia, further validating the reliability of the albedo–NDVI pair, thus reinforcing the model's adaptability. The inability of LST to form a consistently significant correlation with vegetation indices, while unexpected, thus underscores the advantage of the feature-space technique. It filtered out a less reliable indicator (LST in this case) in favor of a more robust one (albedo), leading to a more accurate Desertification Degree Index (DDI).

S/N	Albedo (1999)		LST (1999)	
	Linear Regression	**r**	**Linear Regression**	**r**
1	Albedo = -0.434 NDVI + 0.369	**0.62**	LST = -7.004 NDVI + 31.85	0.23
2	Albedo = -0.386 SAVI + 0.343	0.35	LST = -7.215 SAVI + 31.62	0.16
3	Albedo = -0.328 MSAVI + 0.329	0.30	LST = -7.080 MSAVI + 31.52	0.15
4	Albedo = -0.082 MNDWI + 0.24	0.11	LST = -17.33 MNDWI + 23.53	0.54
	Albedo (2009)		**LST (2009)**	
	Linear Regression	**r**	**Linear Regression**	**r**
5	Albedo = -0.455NDVI + 0.378	**0.51**	LST = 3.709 NDVI + 30.73	0.10
6	Albedo = -0.382 SAVI + 0.356	0.31	LST = 4.537 SAVI + 30.7	0.09
7	Albedo = -0.309 MSAVI + 0.343	0.23	LST = 4.196 MSAVI + 30.782	0.08
8	Albedo = -0.088 MNDWI + 0.267	0.14	LST = 16.418 MNDWI + 25.21	0.62
	Albedo (2024)		**LST (2024)**	
	Linear Regression	**r**	**Linear Regression**	**r**
9	Albedo =-0.279 NDVI + 0.323	**0.63**	LST = -3.455 NDVI + 38.85	0.18
10	Albedo = -0.322 SAVI + 0.316	0.44	LST = -4.128 SAVI + 38.79	0.13
11	Albedo = -0.302 MSAVI + 0.306	0.39	LST = -4.565 MSAVI + 38.84	0.14
12	Albedo = 0.207 MNDWI + 0.352	0.37	LST = -7.171 MNDWI + 33.58	0.30

Table 4: Linear regression of albedo and LST versus NDVI, SAVI, MSAVI, and MNDWI for 1999, 2009, and 2024

NOTE: Generated at Confidence Interval of 95% (p-values < 0.05). r = coefficient of correlation. Sample points = 2100.

3.3 Feature-Space Construction

Figures 7 and 8 illustrate the feature-space of albedo versus NDVI of the study area for 1999, 2009, and 2024, and their corresponding schematic diagram. In Figure 7 (A, B, C), the vertical axis is the albedo, which represents surface reflectance (brightness). Low albedo indicates darker surfaces (vegetated soil and absorbs light), while high albedo indicates brighter surfaces (bare soil, sand) under the same vegetation coverage. Similarly, the horizontal axis is the NDVI, which is a measure of vegetation coverage or greenness. Low NDVI indicates sparse or no vegetation, while high NDVI indicates dense vegetation.

To understand the data distribution and the shape of the feature-space, the density is color-coded, the red dots represent few pixels, which indicates low density, while the green and blue represent more pixels, which indicates high density (See Figure 7). The feature-space shows a negative correlation between the

albedo and NDVI. This implies that high NDVI (dense vegetation, which is dark surface) corresponds to low albedo. In the same vein, low NDVI (bare soil, sand, which are bright surfaces) corresponds to high albedo. Therefore, vegetated pixels are clustered at low albedo and high NDVI, which translate to crops, forests; while bare-soil pixels are clustered at high albedo and low NDVI, which translate to bare soil, sand, rock outcrops, degraded land.

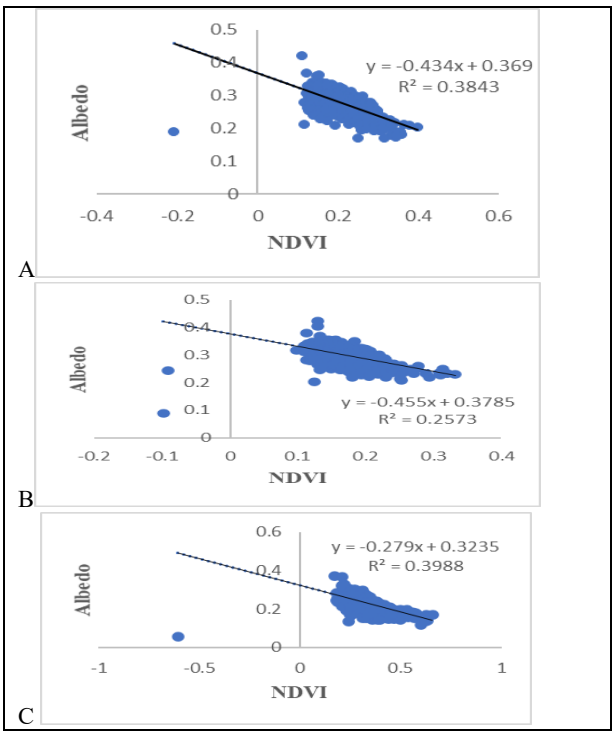

Figure 6: Scatterplots of albedo-NDVI. A: 1999; B: 2009; C: 2024. Note: Sample points = 2100 and p-value = 0.05.

Figure 8 is a schematic diagram, which interprets the feature-space plots. Point A represents region of high albedo with low NDVI, which indicates bright reflectance and is associated with dry bareland, degraded surfaces, meagre or no vegetation. Zone 3, which is in the vicinity of point A reflects conditions of possible desertification. Point C represents region of low albedo with high NDVI and is associated with fully covered land, dense green vegetation, forest, and irrigated crops. Zone 1, which is in the vicinity of point C reflects conditions of no desertification. Point B is between points A and C, represents medium albedo with medium NDVI and is associated with transitional vegetation, sparse vegetation, and degraded land. Zone 2, which is in the vicinity of point B could reflects potential desertification.

The feature-space plots showed a triangle-like shape distribution, which is similar to the feature-space (albedo-NDVI) that was constructed by Ma et al., 2011; Lamqadem et al., 2018; and Salih et al., 2021. Previous studies showed different shapes of feature-space plots. For example, Anh et al. (2006) showed a triangular-like shape for LST vs NDVI; Xulian (2017) showed a trapezium-like shape for Top Soil Grain Size vs NDVI; Wu et al. (2019) showed an arrow-like shape for albedo vs MSAVI; and Wen et al. (2020) showed a trapezium-like shape for albedo vs MSAVI. The difference in the shapes could be as a result of pair of variables used for the feature-space and characteristics of study area.

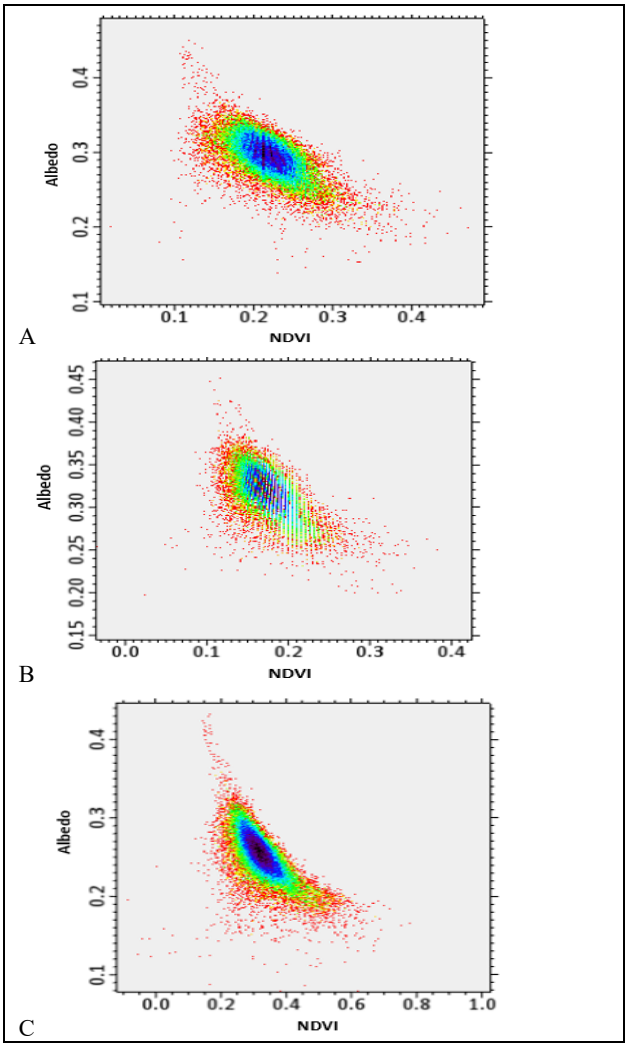

Figure 7: Albedo–NDVI feature-space plots of the study area; A: 1999; B: 2009; C: 2024.

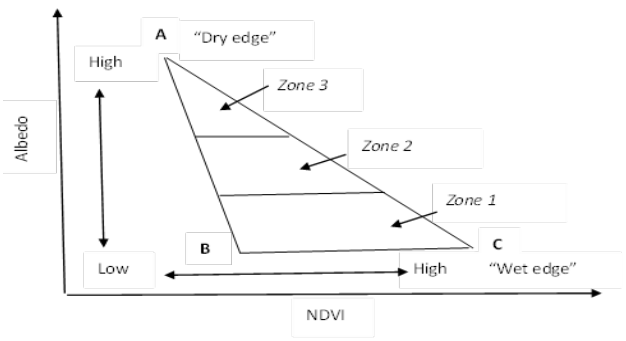

Figure 8: Schematic diagram of Albedo-NDVI feature-space plots.

3.4 Desertification Degree Index (DDI) Classification and Spatio-Temporal Dynamics

Having computed the DDI for the study area to ascertain the desertification degree, Figure 9 (A, B, C) shows the derived DDI maps, which is classified into four classes: desertification, potential desertification, non-desertification (vegetation), and non-desertification (waterbody), Table 5 shows the area extent and percentage area of the DDI maps, and Table 6 presents the

annual expansion rate between successive DDIs. In Figure 9 (A, B, C), the results showed a fluctuating but notable shift in desertification classes over the 25-year period.

The desertification extent, in red colour, occupied an area extent of 34428.69 ha and 18.81% of the study area in 1999, it increased to 37649.16 ha (20.57%) in 2009, and then decreased to 33051.06 ha (18.06%) in 2024. The study area experienced high desertification in 2009 (See Table 5). The land covers attributed to the desertification area are bareland (exposed soils) and rock outcrops. The expansion rate analysis further underscored these dynamics. Between 1999 and 2009, the desertification extent expanded by 0.93% annually, but contracted at 0.81% per year from 2009 to 2024. Overall, desertification area decreased by 0.16% annually from 1999 to 2024 (See Table 6). These changes may reflect efforts of local land management, changing climatic patterns, or natural vegetation recovery.

From visual inspection of the DDI maps in Figure 9, the desertification extent can be seen to be concentrated in the north-east of the study area in 1999, which lies in Mashi area. It signifies that desertification was concentrated in Mashi than Kaita in 1999. The desertification extent can be seen to be concentrated in the north-west (Kaita) and south-east (Mashi) in 2009, and in the north-west (Kaita) in 2024. It can be deduced that the desertification extent was persistent in the north-west of the study area across the study years, thus indicating that Kaita experienced persistent desertification.

The overall decrease of desertification extent from 1999 to 2024 in the study area can be corroborated with the findings of Thlakma and John (2019), who reported a drastic decline of desertification from 43.34% in 1976 to 1.29% in 2006 in Jibia and Kaita LGAs. Though Jibia is westerly of Kaita and Mashi. They attributed the decline of desertification to a mitigation intervention that was carried out by the European Economic Community, Katsina State Government Afforestation Project Unit and Local Government Councils. Despite this mitigation measure, though the persistent desertification underscores ongoing pressures from population growth, overgrazing, farming, erratic rainfall and soil erosion.

The potential desertification class, in light green colour, occupied an area of 73871.19 ha (40.75%) in 1999, it increased to 75825.72 ha (41.44%) in 2009, and then increased to 86611.95 ha (47.33%) in 2024. The land covers attributed to the potential desertification class are cultivated and uncultivated lands. The study area experienced high potential desertification class in 2009. The potential desertification area expanded by 0.26% annually between 1999 and 2009. The potential desertification area also expanded by 0.94% per year between 2009 and 2024, and further expanded by 0.68% annually from 1999 to 2024 respectively. The increase in the potential desertification class across the study years could be attributed to the fact that the inhabitants of the study area earn their livelihood through farming. Therefore, the clearing of vegetation and deforested areas led to cultivated and uncultivated lands. This practice could lead to constant exposure of the soils and could degenerate to bareland if it reaches certain threshold. It is therefore termed potential desertification. These results suggest that while mitigation measures may have curbed outright desertification in some areas, degradation continues to manifest through the expansion of lands that are at risk.

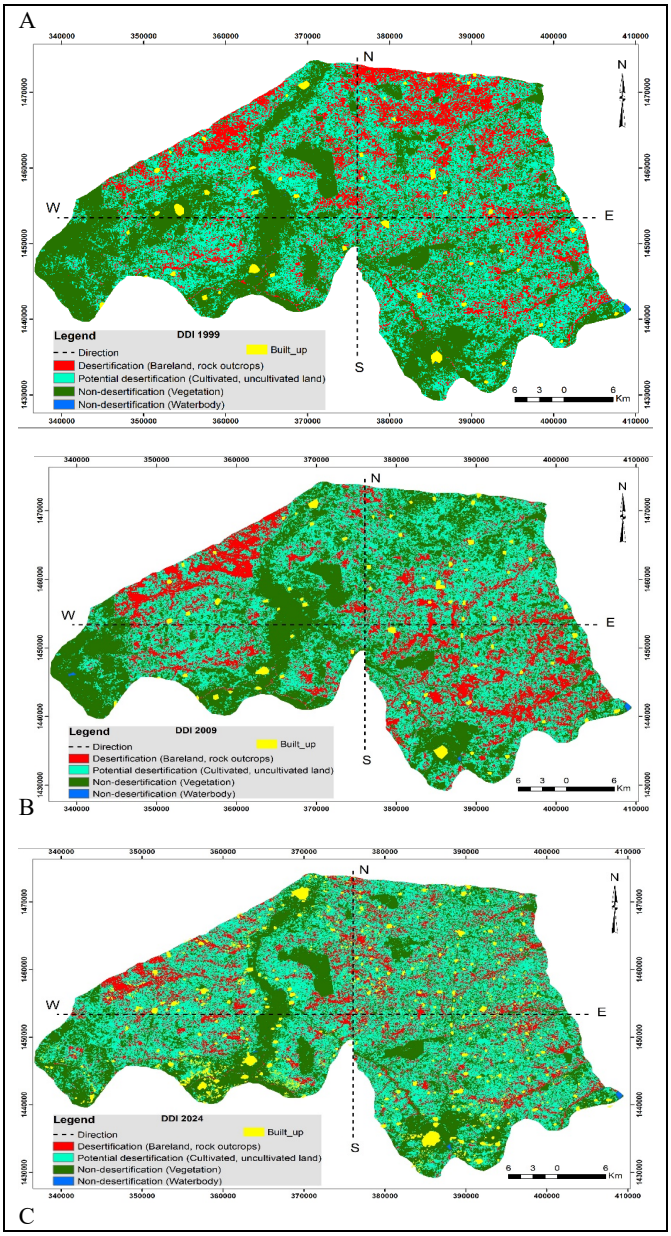

Figure 9: Derived DDI maps from albedo-NDVI feature-space. A: 1999, B: 2009, C: 2024.

The non-desertification class, which is dominated by vegetation and is shown in dark green colour, occupied an area of 74566.53 ha (40.75%) in 1999, it declined to 69395.04 ha (37.92%) in 2009, and then decreased to 63190.08 ha (34.53%) in 2024 respectively. The area of the non-desertification class decreased by 0.69% annually between 1999 and 2009, ollowed by a decline at 0.59% per year between 2009 and 2024, but increased at 0.61% annually from 1999 to 2024. The decline in the non-desertification (vegetation) across the study years underpins the earlier assertion that there has been conversion of the vegetated areas into cultivated and uncultivated lands. Another non-desertification class, which is represented by waterbody occupied 109.98 ha (0.06%) in 1999, it decreased to 106.47 ha (0.05%) in 2009, and then increased to 123.3 ha (0.06%) in 2024. The trend of the waterbody can be attributed to the availability of rainfall for each study year.

Degree	DDI 1999 Area		DDI 2009 Area		DDI 2024 Area	
	ha	%	ha	%	ha	%
Desertification (Bareland, rock outcrops)	34428.69	18.81	37649.16	20.57	33051.06	18.06
Potential desertification (Cultivated, uncultivated)	73871.19	40.37	75825.72	41.44	86611.95	47.33
Non-desertification (Vegetation)	74566.53	40.75	69395.04	37.92	63190.08	34.53
Non-desertification (Waterbody)	109.98	0.06	106.47	0.05	123.3	0.06

Table 5: Area extent and percentage area of the DDI maps for 1999, 2009, and 2024

Degree	DDI 1999 to DDI 2009 (%/year)	DDI 2009 to DDI 2024 (%/year)	DDI 1999 to DDI 2024 (%/year)
Desertification (Bareland, rock outcrops)	**0.9354**	-0.8142	-0.160
Potential desertification (Cultivated, uncultivated)	0.2645	**0.948335**	0.689
Non-desertification (Vegetation)	**-0.6935**	-0.5961	-0.610
Non-desertification (Waterbody)	0.3191	1.053818	0.484

Table 6: Annual expansion rate (%/year) between successive DDIs.

3.5 Validation of DDIs

Having correlated the DDI of 1999, 2009, and 2024 with the SOC, the scatterplots of the relationship between the DDI and SOC for the study years are shown in Figure 10. The scatterplots shows that there is a significant negative correlation between the DDIs and the SOC. While the direction of the correlation is the same for the study years, the strength of the relationships varies. The coefficient of determination of the DDI vs SOC was 0.510, 0.593, and 0.563 in 1999, 2009, and 2024 respectively at a confident interval of 95% p-value of 0.05 (See Figure 10).

The negative correlation of DDI with the SOC was expected. This means that the higher the desertification degree, the lower the SOC content in the soil and vice versa. This validation tested the chemical property of the soil with the DDIs. Therefore, the derived DDIs can be used for the assessment of desertification degree in the study area and can guide mitigation strategy. This validation is corroborated by the validations of Salunkhe et al. (2018) and Wu et al. (2019). The former had negative correlations between Desertification Risk Index (DRI) versus SOM and Cation Exchange Capacity (CEC) in India. The latter also had a negative correlation between Semi-Arid Steppe Desertification Index (SASDI) and Soil Organic Matter (SOM) in China.

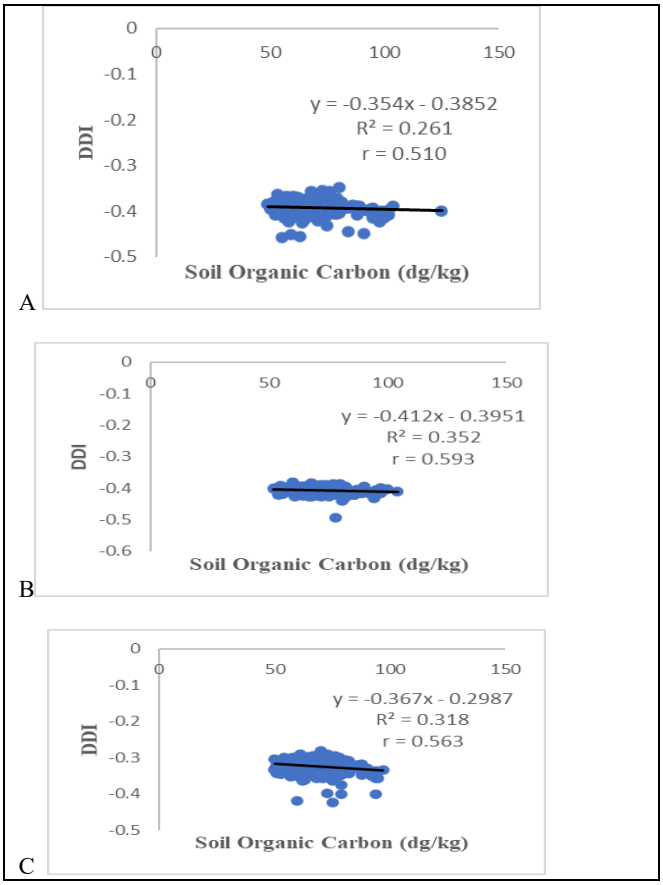

Figure 10: Scatterplots between DDI and Soil Organic Carbon (dg/kg). A: 1999; B: 2009; C = 2024. Note: Sample points = 900 and p-value = 0.05.

3.6 Conclusions

This study set out to address the pressing problem of desertification in northern Nigeria, with a focus on Kaita and Mashi Local Government Areas of Katsina state using albedo–NDVI feature-space. Unlike previous studies in Katsina state that employed techniques like questionnaire-based surveys, land cover classification, and the MEDALUS model, these approaches often generalized northern Katsina as a single zone, relied on indicators without first establishing their local strength of correlation. The feature-space approach has not been explored in Katsina state and Nigeria. This study therefore applied a spatio-temporal albedo–NDVI based feature-space approach to derive and validate Desertification Degree Index (DDI) maps for 1999, 2009, and 2024. The findings revealed that while outright desertification declined slightly after 2009, potential desertification expanded steadily, which was driven largely by the conversion of vegetation to cultivated land. The spatial persistence of desertification hotspots in Kaita underscores localized vulnerability. The study demonstrates the applicability of the feature-space approach in Katsina and Nigeria. It identifies location-specific areas (north-western Kaita) under persistent pressure, thus allowing for focused conservation efforts.

The study theoretically advances and confirms that the albedo-NDVI feature-space, which has been used elsewhere, is also robust and valid in the context of Northern Nigeria. This approach contributes to field of desertification assessment by demonstrating that feature-space indices can be directly linked

with Soil Organic Carbon. More so, the study (maps) can help the Katsina state government and other non-governmental organizations to target reforestation programs specifically in the high-risk north-western zone (Kaita), thus ensuring efficient use of resources. The methodology can be adopted by a national government (e.g., the Nigerian Ministry of Environment) to assess desertification across all frontline states. Despite its contributions, this study has certain limitations. The spatial resolution of Landsat (30m cell size) may miss fine-scale desertification processes. Furthermore, the soil data (SOC) used for validation was sourced from a global model (SoilGrids) rather than from field sampling specific to the study area, which would have provided even more robust ground-truthing. Nevertheless, these choices ensure decadal spatio-temporal assessment and ground-truthing in the absence of field sampled data. Lastly, the study mainly analyzed biophysical indicators, but socioeconomic drivers of desertification such as population growth, land use practices, grazing intensity were not directly integrated. Though focusing on biophysical indicators first was necessary for environmental assessment.

Future study should therefore integrate high-resolution imagery data to enhance the detection of fine-scale degradation features. The incorporation of socio-economic drivers (e.g., population density, grazing intensity) to provide a more holistic understanding of the causal mechanisms behind the observed desertification patterns should be explored. Finally, the assessment of desertification degree, which this study has attempted, is necessary and vital to combating desertification.

Acknowledgements

The authors would like to acknowledge the U. S. Geological Survey and the Soilgrids.org for the provision of the Landsat imagery and the Soil Organic Carbon for this study. The authors also thank the editor of the ASPRS Symposium and the anonymous reviewers during the revision process.

References

Abdulrashid, L. 2017. Farmers' Perceptions of Drivers of Desertification and their Impact on Food Security in Northern Katsina State. *International Journal of Innovative Environmental Studies Research*. 5 (2), 17–27.

Adamo S. B., Crews-Meyer K A., 2006. Aridity and desertification: exploring environmental hazards in Jachal, Argentina. *Appl Geogr.* ;26:61e85.

Aliyu, A. O., 2015. Mapping, Modelling and Analysis of Desertification in Sokoto State, Nigeria. [Masters Dissertation – Departments of Geomatics, Ahmadu Bello University, Zaria Nigeria]. Unpublished.

Aliyu, A. O., Isioye, O. A., Akomolafe, E. A., Abubakar, A. Z. and Abayomi, S. T., 2019. Assessment of Forest Condition In Tangaza West Forest Reserve Area, Gudu Lga, Sokoto State, Nigeria. *Environ*, 4 (8), 68-88 (Print).

Aliyu, A. O., Youngu, T. T., Bala, A., Azua, S., Bawa, S. and Agboola, M. K., 2022. Relationship of the Seasonal Vegetation Indices against the NDVI and LST in the Region of Kamuku Game Reserve and Kwiambana National Park, Nigeria. *Indonesian Journal of Earth Sciences*, 2 (2): 203-225.

Anh, H. V., Williams, M. and Manning, D., 2006. Remote-Sensing Monitoring of Desertification using ASTER and ENVISAT ASAR: Case Study at Semi-Arid Area of Vietnam. International Symposium on Geoinformatics for Spatial Infrastructure Development in Earth and Allied Sciences. Available at: scholar.google.com/citations?user. Retrieved on: 15 September, 2022.

Bouabid, R., Rouchdi, M., Badraoui, M., Diab, A. and Louafi, S., 2010. Assessment of land desertification based on the MEDALUS approach and elaboration of an action plan: The case study of the Souss River Basin, Morocco. In Land Degradation and Desertification: Assessment, Mitigation and Remediation; *Springer*: Dordrecht, The Netherlands, 131–145.

Boutallaka, M., El Mazi, M., Ben-Brahim, Y. and Houari, A., 2023. Mapping the sensitivity of land degradation in the Ouergha catchment (Morocco) using the MEDALUS approach. *Eurasian Journal of Soil Science*, 12 (3): 257-266.

Boutallaka, M., El Mazi, M., Ben-Brahim, Y. and Houari, A., 2023. Mapping the sensitivity of land degradation in the Ouergha catchment (Morocco) using the MEDALUS approach. *Eurasian Journal of Soil Science*, 12 (3): 257-266.

Carlson, T. N., & Ripley, D. A., 1997. On the relation between NDVI, fractional vegetation cover, and leaf area index. *Remote sensing of Environment*, 62 (3), 241-252. https://doi.org/10.1016/S0034-4257(97)00104-1.

De Pina Tavares, J., et al., 2014. Assessment and Mapping the Sensitive Areas to Desertification in an Insular Sahelian Mountain Region: Case Study of the Ribeira Seca Watershed, Santiago Island, Cabo Verde. *Catena*, http://dx.doi.org/10.1016/j.catena.2014.10.005.

Deng, 2014. A ratio normalized difference soil index for remote sensing of urban/suburban environments. https://www.sciencedirect.com/science/article/abs/pii/S0303243415000422.

Ding, J., Yuan, Y. and Fei, W., 2014. Detecting soil salinization in arid regions using spectral feature space derived from remote sensing data. *Acta Ecol Sin*, vol. 34 (16), pp: 4620–4631.

Elijah, H. Ikusemoran, M., Nyanganji, K. J. & Mshelisa, H. U., 2017. Detecting and Monitoring Desertification Indicators in Yobe State, *Nigeria. Journal of Environmental Issues and Agriculture in Developing Countries*, 9 (1).
Falaki, M. A., Ahmed, H. T. & Akpu, B. (2020). Predictive modeling of desertification in Jibia Local Government Area of Katsina State, Nigeria. *The Egyptian Journal of Remote Sensing and Space Science*, 23 (3): 363-370. https://doi.org/10.1016/j.ejrs.2020.04.001.

Guo, B., Han, B., Yang, F., Fan, Y., Jiang, L., Chen, S., Yang, W., Gong, R. and Liang, T., 2019. Salinization Information Extraction Model Based on VI–SI Feature Space Combinations in the Yellow River Delta Based on Landsat 8 OLI Image. *Geomatics Nat Hazards Risk*, vol. 10 (1), pp: 1863–1878.

Ha, T. and Wang, M. X., 2014. Research progresses on the interaction between desertification and climate change in arid and semiarid East Asia. Prog Geogr, vol. (33), pp: 841–852.

Haboudane, D., Miller, J. R., Pattey, E., Zarco-Tejada, P. J., & Strachan, I. B., 2004. Hyperspectral vegetation indices and novel algorithms for predicting green LAI of crop canopies: modeling and validation in the context of precision agriculture. *Remote Sensing of Environment*, 90(3), 337-352. https://doi.org/10.1016/j.rse.2003.12.013.

Hellden, U., 2003. Desertification and Theories of Desertification Control: A Discussion of Chinese and European Concepts. In S. Guangchang (Ed.), Proceedings of the China-EU Workshop on Integrated Approach to Combat Desertification (94-104). Ministry of Science and Technology of China, Chuuina Association for international Sciences 3 and Technology Cooperation.

Hansen, M. C., Potapov, P. V., Moore, R., Hancher, M., Turubanova, S. A., Tyukavina, A., ... & Townshend, J. R. G., 2013. High-resolution global maps of 21st-century forest cover change. *Science*, 342 (6160), 850–853.

James, G. K., Jega, I. M., Halilu, A. S., Olojo, O. O., Oyewunmi, A. S., Shar, J. T., Onuoha, H., Victor, S. et al., 2018. Assessment of Environmental Sensitivity to Desertification in Katsina State, *Nigeria. Environment and Ecology Research,* 6 (6): 545-555. DOI: 10.13189/eer.2018.060604.

Ladisa, G., Todorovic, M. and Liuzzi, G. T., 2012. A GIS-based approach for desertification risk assessment in Apulia region, SE Italy. *Phys Chem Earth*, 49:103-13.

Karnieli, A., Kaufman, Y. J., Remer, L., Dagan, G., and Dashevsky, Z., 2010. Use of NDVI and Land Surface Temperature for Drought Assessment: Merits and Limitations. *Journal of Climate*, 23(3), 618-633. https://doi.org/10.1175/2009JCLI2900.1.

Kennedy, R. E., Andréfouët, S., Cohen, W. B., Gómez, C., Griffiths, P., Hais, M., ... and Zhu, Z., 2014. Bringing an ecological view of change to Landsat-based remote sensing. *Frontiers in Ecology and the Environment*, 12(6), 339–346.

Lal, R., 2004. Soil carbon sequestration impacts on global climate change and food security. *Science*, 304 (5677), 1623-1627.

Lamqadem, A. A., Saber, H. & Pradhan, B., 2018a. Quantitative Assessment of Desertification in an Arid Oasis Using Remote Sensing Data and Spectral Index Techniques. *Remote Sensing*, vol. 10 (1862), doi:10.3390/rs10121862.

Liang, B. P., Li, Y. & Chen, K. Z. A., 2013. Research on Land Features and Correlation between NDVI and Land Surface Temperature in Guilin City. *Remote Sensing Technology and Application*, 27(3), 429–435.

Ma, Z., Xie, Y., Jiao, J., Li, L. and Wang, X., 2011. The Construction and Application of an Aledo-NDVI Based Desertification Monitoring Model. 10, 2029–2035. https://doi.org/10.1016/j.proenv.2011.09.318.

Mamadu, G. N. and Kuje, A. H., 2016. On Major Environmental Problem of Desertification in Northern Nigeria with Sustainable Efforts to Managing it. *World Journal of Science, Technology and Sustainable Development*, 13(1), 18–30. https://doi.org/10.1108/WJSTSD-06-2015-0035.

Medugu, N. I., Majid, M. R. and Johar, F., 2009. The role of afforestation programme in combating desertification in Nigeria. *International Journal of Climate Change Strategies and Management*, 2 (1): 35-47. DOI 10.1108/17568691011020247.

Musa, H. D. and Shaib, B., 2010. Integrated Remote Sensing Approach to Desertification Monitoring in the Crop-Rangeland Area of Yobe State, Nigeria. *Journal of Sustainable Development in Africa*, vol. 2 (12), pp: 236-241.

National Population Commission (NPC) 2006. Population Census Information. Available at: http:// www.npc.gov.ng. Retrieved on: 23 November, 2022.

Nwafor, J. C., 2006. Environmental Impact Assessment for Sustainable Development. EDPCA Publishers Enugu.

Odiogor, H., 2010. Special Report on Desertification in Nigeria: The Sun Eats Our Land. The Vanguard. Available at: http://www.vanguardngr.com/category/more/environment. Retrieved on: 31 June, 2022.

Ogbue, C., Igboeli, E., Ajaero, C., Ochege, F. U., Yahaya, I. I., Yeneayehu, F., You, Y. and Wang, T., 2024. Remote sensing analysis of desert sensitive areas using MEDALUS model and GIS in the Niger River Basin. *Ecological Indicators*, https://doi.org/10.1016/j.ecolind.2023.111404.

Ongsomwang, S., 2007. Fundamental of Remote Sensing and Digital Image Processing. School of Remote Sensing, Institute of Science, Suranaree University of Technology.

Pashaei, M., Rashki, A. & Sepehr, A., 2017. An Integrated Desertification Vulnerability Index for Khorasan-Razavi, Iran. *Natural Resources and Conservation*, 5 (3): 44-55. DOI: 10.13189/nrc.2017.050302.

Qi, J., Chehbouni, A., Huete, A. R., Kerr, Y. H., & Sorooshian, S., 1994. A modified soil adjusted vegetation index. *Remote Sensing of Environment*, 48(2), 119–126. https://doi.org/10.1016/0034-4257(94)90134-1.

Rawls, W. J., Pachepsky, Y. A., Ritchie, J. C., Sobecki, T. M., & Bloodworth, H., 2003. Effect of soil organic carbon on soil water retention. Geoderma, 116 (1-2), 61-76.

Remigios, M. V., 2010. An Overview of the Management Practices at Solid Waste Disposal Sites in African Cities and Towns. *Journal of Sustainable Development in Africa*, 12(7), 233-239. Retrieved from https://jsd-africa.com/Jsda/V12No7_Winter2010_A/PDF/An%20Overview%20of%20the%20Management.

Rivera-Marin, D., Dash, J. and Ogutu, B., 2022. The Use of Remote Sensing for Desertification Studies: *A Review*. 206 (104829). https://doi.org/10.1016/j.jaridenv.2022.104829.

Sajib, M. Q. U. and Wang, T., 2020. Estimation of Land Surface Temperature in an Agricultural Region of Bangladesh from Landsat 8: Intercomparison of Four Algorithms. *Sensors*, 20 (1778). Doi:10.3390/s20061778.

Salvati, L., Zitti, M. and Perini, L., 2016. Fifty years on: Long-term patterns of land sensitivity to desertification in Italy. *Land Degradation and Development*, 27 (2): 97–107.

Salih, A., Hassaballa, A. A. and Ganawa, E., 2021. Mapping Desertification Degree and Assessing its Severity in Al-Ahsa Oasis, Saudi Arabia, using Remote Sensing-Based Indicators. *Arabian Journal of Geosciences*, vol. 14 (192), https://doi.org/10.1007/s12517-021-06523-7.

Salunkhe, S. S., Bera, A. K., Rao, S. S. and Venkataraman, V. R., Raj, U. and Krishna Murthy, Y. V. N., 2018a. Evaluation of Indicators for Desertification Risk Assessment in Part of Thar Desert Region of Rajasthan using Geospatial Techniques. *Indian Academy of Sciences*, 127:116. https://doi.org/10.1007/s12040-018-1016-2.

Saulawa, B. G., Atlhopheng, J., Darkoh, M. B. K., and Mosetlhi, B., 2018. Impact of Desertification on Livelihoods in Katsina State, Nigeria. *Journal of Agriculture and Life Sciences*, 5 (1), 34–52. https://doi.org/10.30845/jals.v5n1a5.

Sepehr, A., Hassanli, A. M., Ekhtesasi, M. R. & Jamali, J. B., 2007. Quantitative Assessment of Desertification in South of Iran using MEDALUS Method. Environ. *Monit. Assess,* 134: 243–254. http://dx.doi.org/10.1007/s10661-007-9613-6.

Sjostrom, M. and Eklundh, L., 2004. Investigating Vegetation Changes in the African Sahel 1982-2002: A Comparative Analysis using Landsat, MODIS and AVHRR *Remote Sensing Data*. Seminar series nr 106. Lund University.

Sun, D., and M. Kafatos, 2007. Note on the NDVI-LST Relationship and the Use of Temperature-Related Drought Indices over North America. Geophys. *Res. Lett*., vol. 34, L24406, doi:10.1029/2007GL031485.

Tanimu, H., 2006. Physical Planning Inputs in Managing Desertification. Project Report, Department of Urban and Regional Planning, Ahmadu Bello University, Zaria Nigeria. Unpublished.

Tercula I., *2015*. Desertification: Water Scarcity hits Sokoto Farmers. Daily Trust. Available at: https://dailytrust.com/desertification-water-scarcity-hits-sokoto-farmers/. Retrieved on: 31 June, 2023.

Thlakma, R. S. and John, O. E.., 2019. An Assessment of The Various Mitigation Strategies to Combat Desertification in Jibia and Kaita Local Government Areas of Katsina State. Geosfera Indonesia, 4 (2): 124-145. 10.19184/geosi.v4i2.10192.

United Nations Convention to Combat Desertification, UNCCD, 1994. Elaboration of an International Convention to Combat Desertification in Countries Experiencing Serious Drought and Desertification particularly in Africa.

United Nations Convention to Combat Desertification, UNCCD, 2022. UNCCD 15th Session of the Conference of the Parties. Available at: https://www.unccd.int/cop15. Retrieved on: 5 December, 2022.

Wei, H., Wang, J., Cheng, K., Li, G., Ochir, A., Davaasuren, D. and Chonou. S., 2018. Desertification Information Extraction Based on Feature Space Combinations on the Mongolian Plateau. *Remote Sensing*, vol. 10 (1614). doi:10.3390/rs10101614.

Wen, Y., Guo, B., Zang, W., Ge, D., Luo, W. and Zhao, H., 2020. Desertification detection model in Naiman Banner Based on the Albedo-Modified Soil Adjusted Vegetation Index Feature Space using the Landsat8 OLI Images. *Geomatics, Natural Hazards and Risk*, vol. 11 (1), pp: 544-558, DOI: 10.1080/19475705.2020.1734100.

Wijitkosum, S., 2016. The impact of land use and spatial changes on desertification risk in degraded areas in Thailand. *Sustainable Environment Research*. http://dx.doi.org/10.1016/j.serj.2015.11.004.

Wu, Z., Lei, S., Bian, Z., Huang, J. and Zhang, Y., 2019. Study of the Desertification Index Based on the Albedo-MSAVI Feature Space for Semi-Arid Steppe Region. *Environmental Earth Sciences*, vol. 78 (232). https://doi.org/10.1007/s12665-019-8111-9.

Xu, H., 2006. Modification of Normalized Difference Water index (NDWI) to enhance open water features in remotely sensed imagery. *International Journal of Remote Sensing*, 27(14), 3025–3033. https://doi.org/10.1080/01431160600589179.

Xulian, B., 2017. Analysis of Desertification Situation Using Remote Sensing and GIS –A Case Study in Ongniud Banner, Horqin Sandy Land. Chiba University – China. Available at: https://opac.ll.chiba-u.jp › curator › SAA_0010. Accessed on: 5 August, 2025.

Yang, H., Gao, F., Zhang, X., & Sun, L., 2022. A review of albedo product development: Progress, challenges, and future perspectives. *Remote Sensing of Environment*, 271, 112907. https://doi.org/10.1016/j.rse.2022.112907.

Yelwa, S. A. & Eniolorunda, N. B., 2012. Simulating the Movement of Desertification in Sokoto and its Environs, Nigeria using 1km SPOT-NDVI Data. *Environmental Research Journal*, 6, 175-181. http://dx.doi.org/10.3923/erj.2012.175.181.

Yusuf, R. T. and Alkhaqani, I. T. H., 2020. Desertification Detection by NDVI and Other Indices: A Case Study in Najaf. Journal of Xidian University, vol. 14 (9), pp: 1148 – 1161. Doi: https://doi.org/10.37896/jxu14.9/126.

Zhao, H., and Chen, X., 2005. Use of normalized difference bareness index in quickly mapping bare areas from TM/ETM+. In Geoscience and Remote Sensing Symposium, 2005. IGARSS'05. Proceedings. 2005 IEEE International, 3: 1666-1668.

Zhu, Z., and Woodcock, C. E., 2014. Continuous change detection and classification of land cover using all available Landsat data. *Remote Sensing of Environment*, 144, 152–171.

Zeng, Y. N., Xiang, N. P., Feng, Z. D. and Hu, H., 2006. Albedo-NDVI space and remote sensing synthesis index models for desertification monitoring. *Sci Geogr Sina*. 26:75–81.

Zielckie, J., 2018. United Nation Support Plan for the Sahel: Working Together for a Prosperous and Peaceful Sahel. Available at: https://reliefweb.int › report › Burkina Faso › un-supp.... Retrieved on: 20 November, 2022.